Cellular Signalling 64 (2019) 109415

Contents lists available at ScienceDirect

Cellular Signalling

journal homepage: www.elsevier.com/locate/cellsig

KDM3A inhibition modulates macrophage polarization to aggravate post-MI injuries and accelerates adverse ventricular remodeling via an IRF4 signaling pathway

Xiaopei Liu, Jing Chen*, Bofang Zhang, Gen Liu, Hongyi Zhao, Qi Hu

Department of Cardiology, Renmin Hospital of Wuhan University, Cardiovascular Research Institute, Wuhan University, Hubei Key Laboratory of Cardiology, Wuhan 430000, China

ARTICLE INFO

Keywords:
KDM3A
Myocardial infarction (MI)
Adverse remodeling
Macrophage polarization

ABSTRACT

It has been reported that KDM3A participates in several cardiovascular diseases through epigenetic mechanisms. However, its biological role post myocardial infarction (MI) has not been explored. Excessive and prolonged inflammation period can aggravate post-MI injuries and accelerates left ventricular (LV) remodeling. Previous studies have shown that macrophages play a momentous role in post-MI injuries by regulating the balance between the inflammatory phase. In this study, we aimed to demonstrate whether KDM3A could regulate the polarization of macrophages to affect the inflammatory response after myocardial infarction and whether targeting KDM3A could influence the prognosis of myocardial infarction and adverse LV remodeling. To explore the biological function of KDM3A and the underlying mechanisms, the loss of function experiments were designed in vitro and vivo. we analyzed the function of macrophages by a phagocytosis and migration assay and explored the polarization of macrophages. The expression of macrophage inflammation-related genes in the acute inflammatory phase and surface markers was detected by western blot and immunofluorescence assays. Echocardiography, Masson's trichrome staining and hematoxylin and eosin (H&E) staining were used to detect cardiac ventricular function. Our data showed that KDM3A is essential for the biological function of rat bone marrow macrophages (BMDMs), and KDM3A deficiency decreases the capacity for phagocytosis and migration, promoting M1 but restraining M2 macrophage phenotype polarization in vitro. Furthermore, we constructed MI models of male rats to verify that KDM3A deficiency could regulate macrophage polarization to aggravate the inflammatory response and accelerate LV remodeling in vivo. Among them, we confirmed that IRF4 is a downstream effector of the KDM3A-dependent pathway which could epigenetically influence the transcription of IRF4 by enhancing histone H3 lysine 9 di-methylation(H3K9me2) accumulation on the IRF4 gene proximal promoter region to modulate macrophage polarization. These results demonstrated that KDM3A plays an essential role in the cardiac repair process of post-MI and LV remodeling by modulating the macrophage phenotype, thereby suggesting a promising therapy to treat post MI injuries.

1. Introduction

Epidemiological research shows that cardiovascular disease is one of the leading causes of morbidity and mortality worldwide. The main pathogenic factors include atherosclerosis, myocardial hypertrophy, myocardial infarction and secondary heart failure [1]. Among these, acute myocardial infarction (AMI) often occurs as the most serious and fatal manifestation of cardiovascular diseases. During myocardial infarction (MI), ischemic cardiomyocytes lose energy supply to necrosis, the cardiomyocyte death process is activated, and apoptosis and autophagy occur successively. In addition, injured endothelial cells lead to increased vascular permeability, and a series of inflammatory cells infiltrate to enhance the inflammatory response. Finally, those pathological processes directly result in myocardial injury, left ventricular (LV) remodeling and cardiac insufficiency [2]. Although timely reperfusion therapy can effectively alleviate myocardial damage and minimize infarct size, irreversible cardiomyocyte loss in the acute stage of ischemia and the ensuing progressive maladaptive ventricular remodeling still lead to a relatively high incidence of secondary heart failure or even sudden cardiac death [2,3]. Therefore, it is necessary to seek novel effective measures to improve the cardiac repair process after myocardial infarction.

* Corresponding author.
E-mail address: chenjing821111@163.com (J. Chen).

https://doi.org/10.1016/j.cellsig.2019.109415
Received 1 July 2019; Received in revised form 8 September 2019; Accepted 8 September 2019
Available online 09 September 2019
0898-6568/

Cardiac repair after infarction proceeds through three stages, and macrophages play different roles at each stage [1,3]. The first stage of cardiac repair is the inflammatory stage of postinfarction repair. In this stage, macrophages mainly exhibit the M1 proinflammatory phenotype and secrete IL-1β, IL-6, TNF-α and MMP-9 to facilitate phagocytosis and proteolytic and inflammatory responses. However, an excessive inflammatory response is not conducive to the repair of necrotic myocardium in the later stages [4,5]. The second stage of cardiac repair is the postinfarction repair and proliferation phase. In this stage, inflammation is dissipated and apoptotic neutrophils are swallowed by macrophages, which change to the reparative M2 phenotype and exert an anti-inflammatory effect, releasing TGF-β and IL-12 to accelerate angiogenesis and activate myofibroblasts to form collagen-rich scars [4,6]. The last stage of cardiac repair is the postinfarction repair maturation stage. In this stage, M2 macrophages stimulate the synthesis of extracellular matrix (ECM), which is crosslinked in the infarct area, covering the necrotic cardiomyocytes and providing a skeleton for the cells to regulate their various activities in the process of tissue repair. Repaired cells are inactivated, myofibroblasts are stationary, and the newly formed scar matures gradually [6]. Therefore, macrophages play a momentous role in regulating the balance between the inflammatory phase and the repair phase. Indeed, M2 macrophages have a greater influence than M1 macrophages on the pathological progression of infarction tissue, improving the prognosis of myocardial ischemic infarction [7]. More effective, timely repair can alleviate post-MI injuries and poor left ventricular remodeling.

Histone lysine demethylase KDM3A (also known as JMJD1A and JHDM2A) is a member of the Jumonji C domain-containing histone demethylase family and promotes the demethylation of H3K9me2 (dimethylated histone H3 at lysine 9) and H3K9me1 (monomethylated histone H3 at lysine 9) to regulate gene expression [7,8]. Previous studies have confirmed that KDM3A plays an active role in metabolism and sperm formation. In addition, it has been reported that KDM3A can also exacerbate the invasiveness of tumor cells in breast and colorectal cancer, and its presence is deemed a sign of poor prognosis [8–10]. Recently, emerging studies have verified that KDM3A is involved in an important epigenetic mechanism in cardiovascular diseases, such as diabetic cardiomyopathy [11], myocardial infarction [12] and cardiac hypertrophy [13]. Our previous studies found that KDM3A regulated smooth muscle cell function in a high-glucose environment and vascular remodeling in diabetes mellitus; the underlying mechanism was that KDM3A could regulate the inflammatory response [14,15]. According to these findings, we conclude that KDM3A may play a central role in the inflammatory response of the cardiovascular system. In addition, because macrophages play a key role in inflammatory repair after myocardial infarction.

Thus, in the present study, we aimed to demonstrate whether KDM3A could regulate the polarization of macrophages to affect the inflammatory response after myocardial infarction and whether targeting KDM3A could influence the prognosis of myocardial infarction and adverse LV remodeling. To explore the biological function of KDM3A and the underlying mechanisms, we examined the impact of KDM3A on the biological function of rat bone marrow macrophages (BMDMs) in vitro. We also constructed models of rat MI to explore whether KDM3A can regulate macrophage polarization to affect post-MI injuries and ventricular remodeling in vivo. In addition, we investigated the underlying mechanisms of this regulation.

2. Materials and methods

2.1. Cell culture

The BMDMs used in this study were obtained from the bone marrow cells of syngeneic adult, male SD rats as previously described [16]. In brief, the rats were sacrificed; their femurs and tibias were removed after alcohol disinfection; the bone marrow was collected, filtered through a 70 μm strainer (BD falcon), and centrifuged for 5 min at 1000 rpm; and the cells obtained were cultured on petri dishes in RPMI-1640 medium (HyClone; GE Healthcare Life Sciences) supplemented with 10% fetal bovine serum (FBS; Gibco; Thermo Fisher Scientific, Inc), 20 ng/ml macrophage colony stimulating factor (M-CSF; PeproTech; 400-28) and 1% penicillin/streptomycin (HyClone; Ge Healthcare Life Sciences). After 3 days, the medium in the petri dishes was replaced with fresh medium with the same concentration of M-CSF. The BMDMs that were differentiated for 5–7 days were used for the experiment.

For macrophage polarization, the BMDMs were incubated with 1 μg/ml LPS for 24 h (Sigma; L2880) to be polarized as M1 macrophages and were incubated with 20 ng/ml IL-4 (PeproTech; 400-04) for 24 h to be polarized as M2 macrophages.

2.2. Identification of cell phenotypes

For phenotype identification, cells were detected by anti-F4/80 and anti-CD68 antibodies in an immunofluorescence costaining experiment [17]. Briefly, after differentiation for 5–7 days, the cells were fixed with 4% paraformaldehyde for 30 min and then washed with PBS 3 times for 5 min. After blocking in 5% normal goat serum for 1 h at room temperature, cells were labeled with anti-F4/80 (Bioss, bs-11182R) and anti-CD68 antibodies (NOVUS, NB100-683) and then incubated with the appropriate secondary antibodies, including FITC-conjugated goat anti-rabbit IgG (Aspen, AS-1110) and Cy3-conjugated goat anti-mouse IgG (Aspen, AS-1111). Finally, nuclei were stained with 4′,6-diamidino-2-phenylindole (DAPI, Sigma), the images were viewed with a fluorescence microscope (OLYMPUS IX51, Tokyo, Japan), and differentiated BMDMs were costained with anti-F4/80 and anti-CD68 antibodies.

2.3. Adenovirus construction and transfection

Adenovirus encoding KDM3A-shRNA (AdshKDM3A) was constructed by Genechem (Shanghai, China), and AdshRNA was used as a negative control. These viruses were applied in our previous studies and were shown to effectively induce the knockout of KDM3A in vitro [13,14]. The most suitable multiplicity of infection (MOI) of adenovirus transfection was determined to be 40 in pre-experiment studies. When the density of BMDMs reached 70–80%, they were cultured in serum-free medium for 12 h after transferring adenovirus and then replaced with complete culture medium for another 24–48 h. Forty-eight hours later, the expression of green fluorescent protein in the cells was observed by fluorescence microscopy, and western blot analysis further revealed KDM3A expression. These results showed that the adenovirus was successfully transferred.

2.4. Experimental design

To explore whether KDM3A could affect the function of macrophages, cells in our in vitro experiment were randomly divided into three groups: a) a control group, containing BMDMs without any treatment; b) an AdshRNA group, containing BMDMs infected with AdshRNA; and c) an AdshKDM3A group, containing BMDMs infected with AdshKDM3A. Rats were randomly divided into four groups for our in vivo experiments: a) a wild-type rat sham operation group (WT-SO); b) a KDM3A-knockout rat sham operation group (KO-SO); c) a WT-MI operation group; and d) a KO-MI operation group. We analyzed the function of macrophages by a phagocytosis and migration assay and explored the polarization of macrophages. The expression of macrophage inflammation-related genes in the acute inflammatory phase and surface markers was detected by western blot and immunofluorescence assays. Echocardiography, Masson's trichrome staining and hematoxylin and eosin (H&E) staining were used to detect cardiac ventricular function.

2.5. Macrophage chemotaxis assay

Chemotaxis assays were performed in 24-well Transwell plates (Corning, NY, USA) with 8 μm pore-size membrane inserts. To obtain conditioned medium in the lower chamber, oxygen and glucose deprivation (OGD) was applied to simulate myocardial ischemia injury in vivo as previously described [18]. In brief, neonatal rat cardiomyocytes were cultured in serum-free Dulbecco's modified Eagle's medium (DMEM; HyClone; GE Healthcare Life Sciences) and incubated in an atmosphere of 94% N_2, 5% CO_2, and 1% O_2 for 6 h. Subsequently, the supernatant was collected and transferred to the lower chamber of the Transwell plate. BMDMs were collected in 200 μl serum-free RPMI-1640 medium, and the cell suspension was placed into the upper chamber of the plate. The chamber containing cells was incubated for 8 h at 37 °C. At the end of the incubation, the upper-chamber cells had migrated to the lower surface of the membrane. The chamber was removed, and the cells that had not migrated to the lower surface of the membrane were gently wiped with a cotton swab. The chamber with the migrated cells was fixed with methanol for 30 min and stained with 0.5% crystal violet in the dark for 30 min at 25 °C. The ratio of cell migration was determined by a light microscope (Olympus Corporation, Tokyo, Japan) to count the number of migrated cells in five randomly chosen fields.

2.6. Macrophage phagocytosis assay

A phagocytosis assay was performed by analyzing the macrophage engulfment of fluorescent red latex beads (1 mm diameter, L-2778, Sigma Aldrich) as previously demonstrated [19]. Briefly, latex beads were incubated with RPMI-1640 medium for 1 h at 37 °C, added to the BMDMs at a ratio of 10:1, and cocultured at 37 °C for an additional 2 h. At the end of this incubation, the medium was aspirated, and sterile PBS was used to wash away the nonengulfed latex beads. To count the rate of phagocytosis, cells were stained with phalloidin. The cells were fixed with 4% paraformaldehyde (PFA) for 10 min. The actin cytoskeleton was stained with phalloidin for 30 min in the dark. Next, nuclei were stained with DAPI for 2 min. After washing with PBS, stained cells were examined by fluorescence microscopy (OLYMPUS IX51, Tokyo, Japan), and the number of engulfed beads was counted in five randomly chosen fields.

2.7. Animals

Our study was approved by the Institutional Animal Care and Ethics Committee of the Renmin Hospital of Wuhan University (20140305) and followed the institutional guidelines of the Institutional Review Board. All of the male Sprague-Dawley (SD) rats (SPF grade, 200–250 g) were provided by Wuhan University Experiment Animal Center. Regarding the genetic deletion of KDM3A, CRISPR/Cas9 genome-editing technology [20] was used to generate a KDM3A-knockout (KO) rat (SD background).

2.8. Myocardial infarction models

Myocardial infarction (MI) was evoked by permanent ligation of the left anterior descending coronary artery (LAD) as described in previous studies [21]. Briefly, adult SD rats (male, 200–250 g) were anesthetized by an intraperitoneal injection of 3% sodium pentobarbital (60 mg/kg) and artificially ventilated with an animal ventilator through a tracheal cannula. An electrocardiograph was used to continuously monitor the standard body ECG. Next, a left thoracotomy was performed in the 4th left intercostal space. MI was induced by permanent ligation of the LAD proximal to its bifurcation from the main stem with 6-0 silk suture, and a successful MI model was confirmed by an elevated ST segment in lead II and a pale region of the myocardial surface. At the end of surgery, the chest was sutured. Rats in the sham group were subjected to the same surgical procedures except for LAD artery ligation. The hearts were harvested and perfused with ice cold saline. For western blot analysis and immunostaining studies, infarct/border zone tissue was separated from the hearts. For Masson's trichrome staining and histopathological examination after 7 days, whole hearts were retained.

2.9. Echocardiography

Transthoracic echocardiography was performed on rats that were preanesthetized by isoflurane and then transferred to an ultrasonic platform. During echocardiographic examinations, the rats' heart rates were continuously monitored. The major items measured included left ventricular (LV) ejection fraction (LVEF) and LV fractional shortening (LVFS). Images were acquired from the parasternal short axis at the midlevel of the papillary muscle, and at least three separate cardiac cycles were measured by a MyLab 30CV ultrasound system (Biosound Easote, Inc.).

2.10. Histopathological examination

A week after MI surgery, rats from all groups were anesthetized, and the cardiac samples were collected and fixed in 4% paraformaldehyde at 4 °C for 24 h, followed by paraffin embedding. Sections of 5 μm thickness were taken every 100 μm at the plane of the papillary muscle. Next, Masson's trichrome staining and hematoxylin & eosin (H&E) staining were performed following the manufacturer's protocol. Thereafter, images were taken with a PathScan Enabler IV slide scanner. The percentage of infarct size of each section and the degree of myocardial injury were calculated.

2.11. Immunofluorescence analysis

Immunofluorescence analysis was performed as previously described [22]. In brief, one week after MI surgery, rats from all groups were anesthetized, and hearts were quickly harvested and washed with cold normal saline to eliminate residual blood in the heart. The infarct/border zone was then separated, fixed with 4% PFA solution for 24 h, and embedded in paraffin for immunofluorescence analysis. Transversal sections (5 μm thickness) were prepared every 100 μm.

2.12. Western blot analysis

Following the designated treatment, myocardial tissues were minced, homogenized and digested in tissue lysis buffer, and the BMDMs were lysed with RIPA. The protein suspensions were collected, and the protein concentration was determined by a BCA kit. Total proteins were then separated by PAGE gel electrophoresis and transferred to PVDF membranes. Subsequently, membranes were incubated with relevant antibodies against CD68 (NOVUS, NB100-683), TNF-α (Abcam, ab66579), iNOS (Abcam, ab15323), CD86 (Proteintech, 13395-1-AP), Arg-1 (Santa, sc-271430), Ym-1 (Abcam, ab192029), CD206 (Abcam, ab125028), IRF4 (lsbio, LS-C192325), KDM3A (Abcam, ab106456), and GAPDH (Abcam, ab37168) overnight at 4 °C at an appropriate dilution. The membrane was incubated with the appropriate secondary antibodies. Finally, the results were analyzed with an ECL detection system, and the bands were visualized with an enhanced chemiluminescence system.

2.13. Chromatin immunoprecipitation (ChIP)-PCR

ChIP was performed according to the manufacturer's protocol and ChIP-enriched DNA was detected by real-time PCR as previously depicted. In brief, BMDMs were fixed and cross-liked with 1% formaldehyde for 20 min at room temperature. Cell lysates were sonicated prior to finish cross-linking by 0.125 M glycine for 5 min. Then, the DNA lysates were immunoprecipitated with 5 μg antibody against

H3K9me2 (Abcam) or non-immune IgG (Santa Cruz) for negative control in the presence of magnetic beads with secondary antibody. Immune complexes and input were washed, eluted with buffer. Next, ChIP-enriched DNA samples were isolated and analyzed by real-time quantitative PCR using primers closed to the promoter sites on the IRF4, and ChIP values were normalized as a percentage of Input. The results were expressed as a percentage of Control group.

2.14. Statistical analysis

The results are presented as the mean ± standard deviation. Student's *t*-test was used to compare the data between two groups. ANOVA followed by Bonferroni post hoc analysis was used for comparisons among multiple groups. A P value of < 0.05 was regarded as statistically significant. All statistical analyses were performed with SPSS 19.0 software.

3. Results

3.1. BMDM identification and adenovirus transfection

As shown in Figs. 1A, 7 days after incubation, almost all cells in one random visual field were colabeled with F4/80 (green) and CD68 (red). These results suggested that the cells isolated from the bone marrow of SD rats had exactly differentiated into mature BMDMs. To clarify whether adenovirus was transfected successfully into the macrophages, we first detected the expression of KDM3A in BMDMs by immunofluorescence analysis, and the results showed that KDM3A was expressed in the cytoplasm/nucleus of BMDMs (Fig. 1B). We then confirmed the adenovirus transfection efficiency by fluorescence microscopy and western blotting. We found that BMDMs infected with adenovirus emitted strong green fluorescence, and the expression of KDM3A was significantly downregulated by adenovirus transfection (Fig. 1C–D). These results collectively illustrated that adenoviruses were transfected into BMDMs successfully and that KDM3A expression was attenuated.

3.2. KDM3A inhibition attenuates macrophage phagocytosis and migration capability

We examined the effects of inhibiting KDM3A expression on the major function of macrophages from two aspects: phagocytosis and migration capability. Phagocytosis refers to the absorption and degradation of pathogens by activated macrophages and the clearance of necrotic cells [23]. To detect the effects of inhibiting KDM3A expression on the phagocytotic capability of macrophages, we performed coculture experiments with BMDMs and latex beads. As shown in Fig. 2A–B, the macrophages engulfed the latex beads that were stained with phalloidin, and in the AdshKDM3A group, the phagocytic capability of macrophages was inferior to that of the AdshRNA group, and it was the lowest phagocytic rate among the three groups. The migration capability of macrophages means that when the organism is stimulated and damaged, macrophages will be activated and migrate to the injured site. To study the role of KDM3A in macrophage migration, the supernatant of primary neonatal rat cardiomyocytes cultured in hypoxic and glucose-deficient conditions for 4 h was collected as a chemokine to induce macrophage migration. The migration of macrophages was evaluated in a Transwell chamber. Our data showed that the migration number of macrophages in the AdshRNA group was approximately 4-fold higher than that in the AdshKDM3A group, and there was no significant difference in migration between the AdshRNA group and the control group (Fig. 2C–D), indicating that the downregulation of KDM3A inhibited macrophage migration.

3.3. KDM3A inhibition enhances M1 but suppresses M2 macrophage polarization in cultured BMDMs

To investigate whether KDM3A takes part in regulating the polarization of macrophages, we detected the expression of KDM3A protein in BMDMs treated with LPS (1 μg/ml for M1 macrophages) or IL-4 (20 ng/ml for M2 macrophages) for 24 h. We found that the expression of KDM3A changed perceptibly. In M1-stimulated BMDMs, the expression of KDM3A was lower than that of the control group, while the expression of KDM3A in M2-stimulated BMDMs was higher than that of the control group (Fig. 3A). Because the expression of KDM3A changed during polarization toward M1 and M2 macrophages, we questioned whether KDM3A had an effect on M1 and M2 polarization. We inhibited

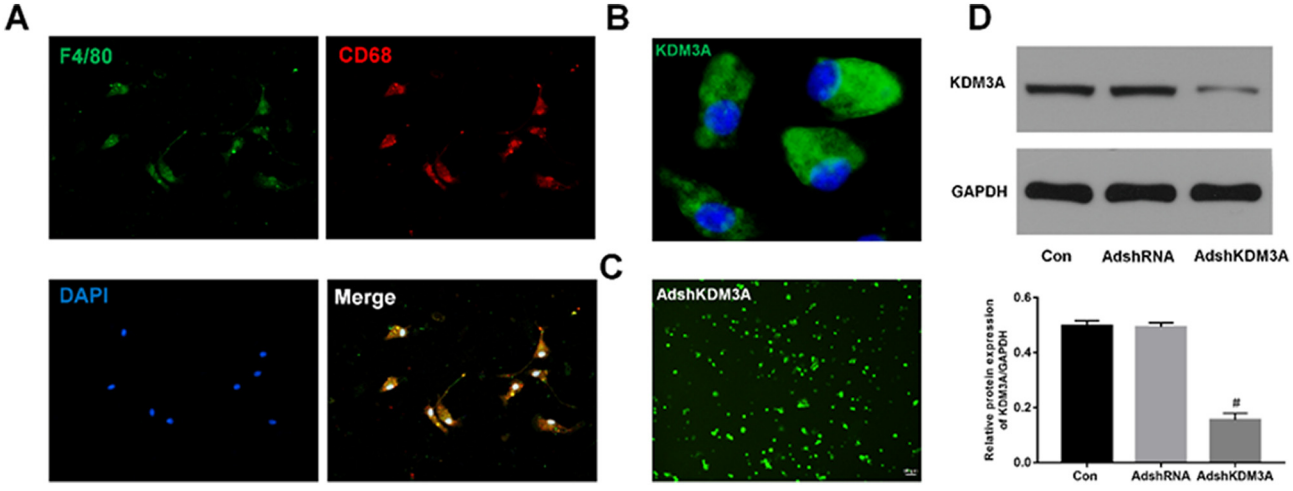

Fig. 1. BMDM identification: transfection of AdshKDM3A suppresses the expression of KDM3A protein in BMDMs.
(A–B) Immunofluorescence costaining of BMDMs surface makers CD68 (red) and F4/80 (green) (×200) and immunofluorescence staining of KDM3A (green) BMDMs seven days after incubation. The nuclei were stained with DAPI (blue), $n = 3$. (C) Representative fluorescence microscopy images after transfection of AdshKDM3A into BMDMs (×100). (D) The expression of KDM3A protein was determined by western blot analysis ($n = 3$). Data are expressed as the mean ± standard deviation, $n = 3$, $^{\#}P < .05$ vs. the AdshRNA group. BMDMs: bone marrow macrophages; KDM3A: lysine (K)-specific demethylase 3A; GAPDH: glyceraldehyde 3-phosphate dehydrogenase; DAPI: 4,6-diamidino-2-phenylindole. (For interpretation of the references to colour in this figure legend, the reader is referred to the web version of this article.)

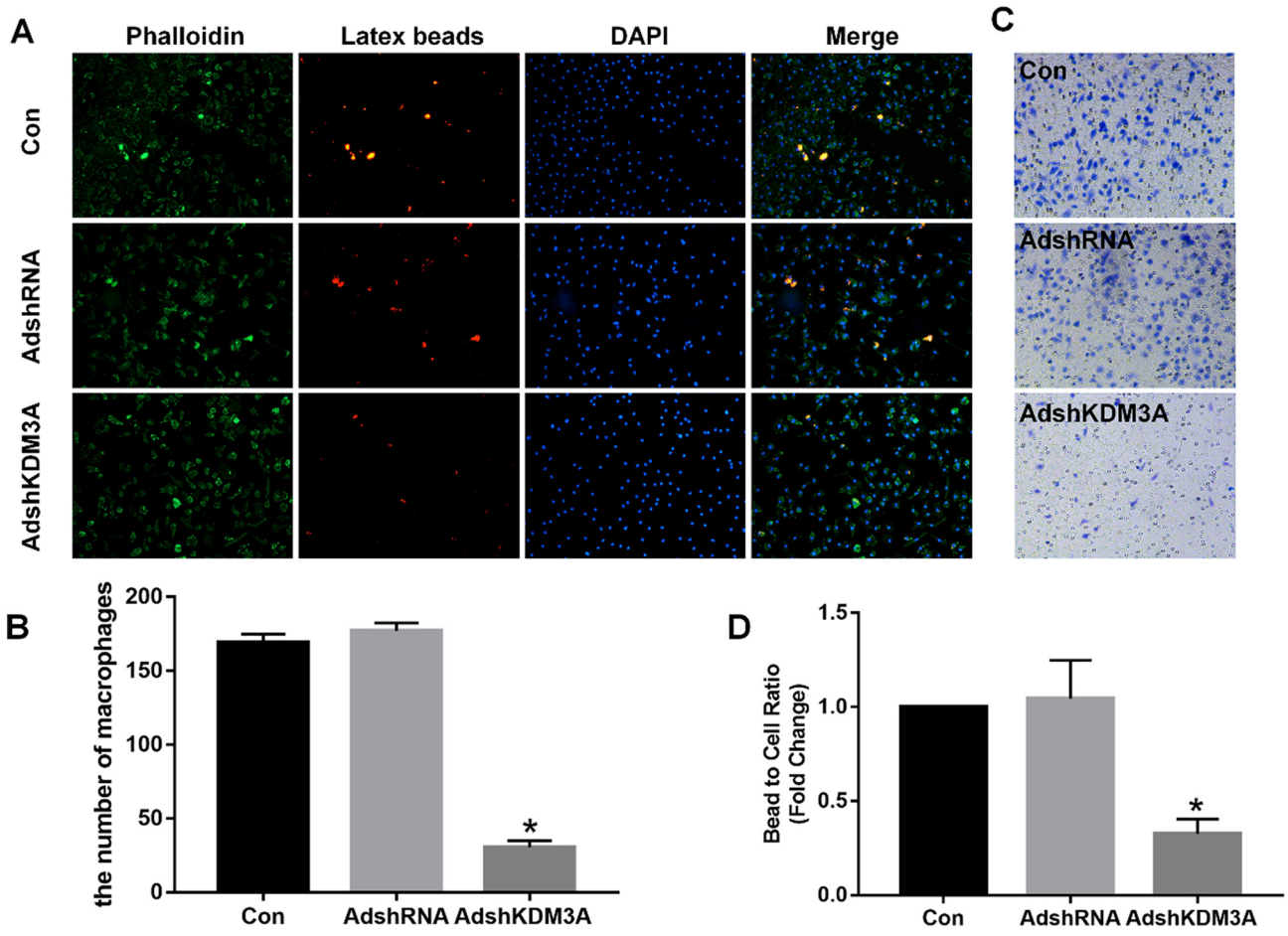

Fig. 2. KDM3A deficiency affects the biological function of macrophages.
(A–B) Representative fluorescence microscopy images of the phagocytosis capability of BMDMs (×200). The ratio of BMDMs engulf the latex beads compared to the control group ($n = 3$). (C–D) Representative images of the effects of KDM3A deficiency on BMDM migration potential (×200) and the number of migrated BMDMs after transduction of adenovirus ($n = 3$). Data are expressed as the mean ± standard deviation, $^*P < .05$ vs. the AdshRNA group. KDM3A: lysine (K)-specific demethylase 3A; BMDMs: bone marrow macrophages.

the expression of KDM3A in the process of inducing polarization of M1 and M2 macrophages and detected the protein marker expression of M1 macrophages (such as TNF-α, iNOS, and CD86) and M2 macrophages (such as Arg-1, Ym-1, and CD206). As shown in Fig. 3B and D, the expression of KDM3A had been inhibited in the process of inducing polarization of M1 and M2 macrophages. The results in Fig. 3C and E show that M1 or M2 macrophage marker protein levels were increased when exposed to stimulators of the microbial inflammatory response, such as LPS or IL-4. However, comparing the macrophage polarization conditions of AdshKDM3A and AdshRNA, KDM3A gene silencing effectively promoted the expression of M1 macrophage marker proteins. At the same time, the expression of M2 macrophage marker proteins was inhibited with IL-4 stimulation.

3.4. KDM3A knockout aggravates the deterioration of cardiac function and adverse remodeling post MI

The protective effect of repaired macrophages on cardiac function, especially the healing of ischemic myocardial wounds, has been widely studied and verified, and the repair effect reached its high peak on the seventh day of ischemic injury [5,24]. We first detected the KDM3A expression by Western-blot to confirm whether it had been generated KDM3A-knockout (KO) rat successfully. As expected, there was no protein expression of KDM3A compared to the WT group (Fig. 4A). Then we verified the effect of KDM3A deficiency on cardiac function after myocardial infarction. The cardiac function of each group was measured by echocardiography, including left ventricular ejection fraction (LVEF) and left ventricular fractional shortening (LVFS) at seven days and one month. As shown in Fig. 4B, the values of LVEF and LVFS in the KO-MI group were lower than those in the WT-MI group on the seventh day and one month after myocardial infarction. Additionally, the WT-SO group and KO-SO group without operation showed no significant differences. Masson's trichrome staining was performed on the infarcted hearts of each group to analyze the infarcted area and collagen deposition volume at 7 days post MI. As shown in Fig. 4C–D, the infarction area of the KO group was larger than that of the WT group, and the density of collagen deposition was higher. The collagen density in the KO group was increased to 29.09 ± 1.891% according to the percentage of collagen area in the total area of the microscopic visual field by quantitative analysis with Image ProPlus software. In Fig. 4E, H & E staining showed that the myofibril structure damaged in the KO group was more serious than that in the WT group, and there was inflammatory cell infiltration. These results suggest that KDM3A not only aggravates left ventricular function but also increases the process of left ventricular remodeling deterioration.

3.5. KDM3A knockout inhibits macrophage polarization from the M1 to the M2 subtype and aggravates inflammatory responses post MI

To determine the effect of KDM3A on the distribution and polarization of cardiac resident macrophages, immunofluorescence staining was performed on the seventh day after infarction. CD86 and CD206

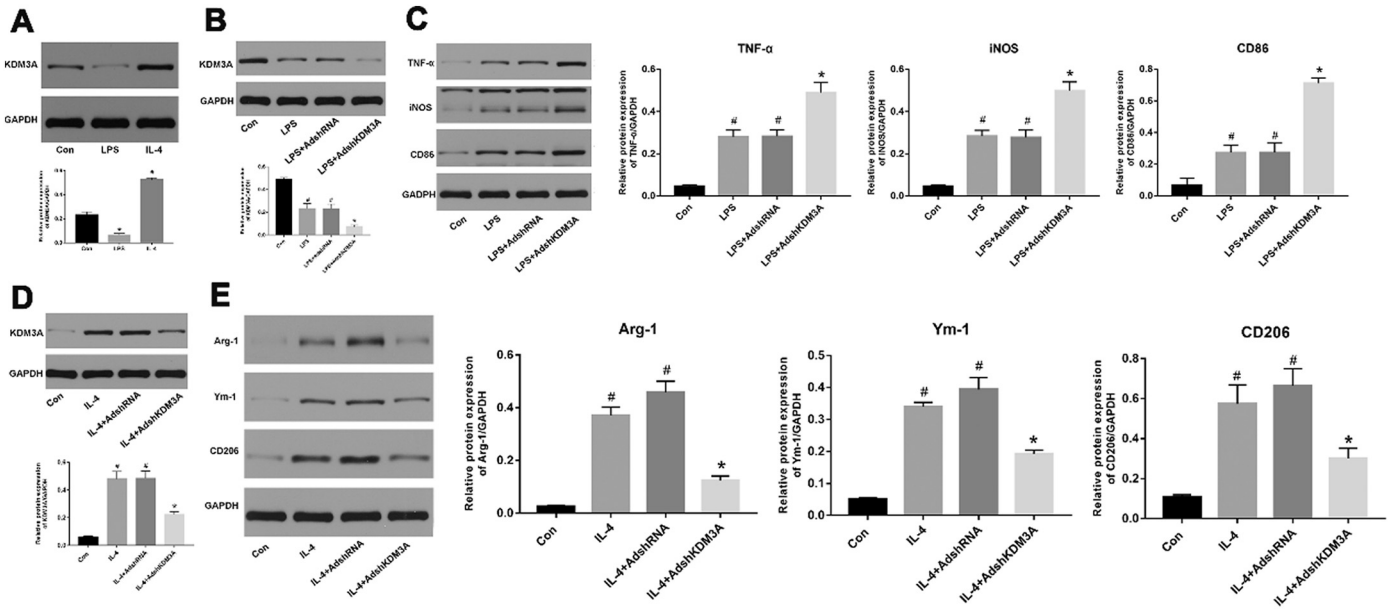

Fig. 3. Expression of KDM3A during M1 and M2 polarization: KDM3A inhibition increases M1 but suppresses M2 macrophage polarization in vitro.
BMDMs were stimulated with medium alone (Con), LPS (1 μg/ml) for M1 polarization and with IL-4 (20 ng/ml) for M2 polarization. (A) KDM3A protein expression was determined by western blot analysis ($n = 3$, $^{\#}{}^{*}P < .05$ vs. the Con group). (B–C) The protein expression of KDM3A and M1 macrophage markers TNF-α, iNOS, and CD86 following transduction of adenovirus ($n = 3$, $^{*}P < .05$ vs. LPS + AdshRNA or LPS, $\#P < .05$ vs. Con) (D-E) The protein expression of KDM3A and M2 macrophage markers Arg-1, Ym-1, and CD206 following transduction of adenovirus ($n = 3$, $^{*}P < .05$ vs. IL-4 + AdshRNA or IL-4, $\#P < .05$ vs. Con). Data are expressed as the mean ± standard deviation. BMDMs: bone marrow macrophages; LPS: lipopolysaccharide; IL-4: interleukin-4; TNF-α: tumor necrosis factor alpha; iNOS: inducible nitric oxide synthase; Arg-1: arginase-1; KDM3A: lysine (K)-specific demethylase 3A; GAPDH: glyceraldehyde 3-phosphate dehydrogenase.

are cell surface markers marking M1 subtypes and M2 subtypes, respectively, and we also detected representative proinflammatory (TNF-α and iNOS) or anti-inflammatory (Arg-1 and Ym-1) markers secreted by macrophages through western blotting. As shown in Fig. 5A, there are a large number of macrophages in the infarction area in the WT-MI and KO-MI groups. $CD86^{+}$ macrophages were more widely distributed in the KO-MI group, while $CD206^{+}$ macrophages were more densely distributed in the WT-MI group (Fig. 5B–C). Furthermore, there was no significant difference between the WT-SO and KO-SO groups, which had few distributed $CD86^{+}$ macrophages or $CD206^{+}$ macrophages. The proportion of $CD86^{+}/CD206^{+}$ macrophages in the infarcted border of the KO-MI group was significantly higher than that in the WT-MI group by quantitative analysis with Image ProPlus software (Fig. 5D). These data indicate that the KO-MI group had more proinflammatory macrophages (M1) than the WT-KO group and that the capability for macrophage polarization from the proinflammatory phenotype (M1) to the reparative phenotype (M2) was diminished. Then, western blot analysis showed that the expression of KDM3A had been suppressed in

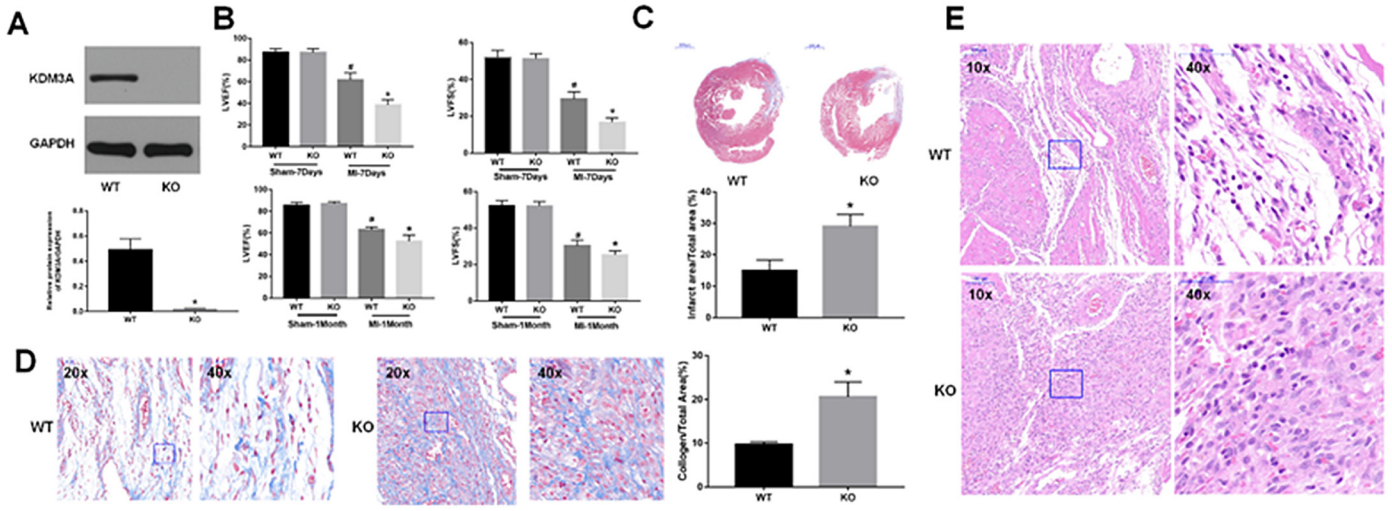

Fig. 4. KDM3A knockout exacerbates cardiac functional and adverse remodeling post MI.
(A) KDM3A protein expression was determined by western blot analysis ($n = 3$, $^{*}P < .05$ vs. the WT group) (B) Statistical analysis of echocardiographic parameters (LVEF and LVFS) indicated left ventricular function at 7 days and one month post MI ($n = 4$, $^{*}P < .05$ vs. WT-MI, $^{\#}P < .05$ vs. sham). (C) Representative Masson's trichrome staining of cardiac papillary muscle cross-section and quantification of the infarct area ($n = 4$, $^{*}P < .05$ vs. WT). (D) Representative Masson's trichrome staining (×200 and ×400) and quantification of collagen area ($n = 4$, $^{*}P < .05$ vs. WT). (E) Representative images of the hematoxylin and eosin (H&E) staining of the MI border zone (×100 and ×400, $n = 4$). Data are expressed as the mean ± standard deviation. LVEF: left ventricular ejection fraction; LVFS: left ventricular fractional shortening; MI: myocardial infarction; WT: wild-type; KO: knockout.

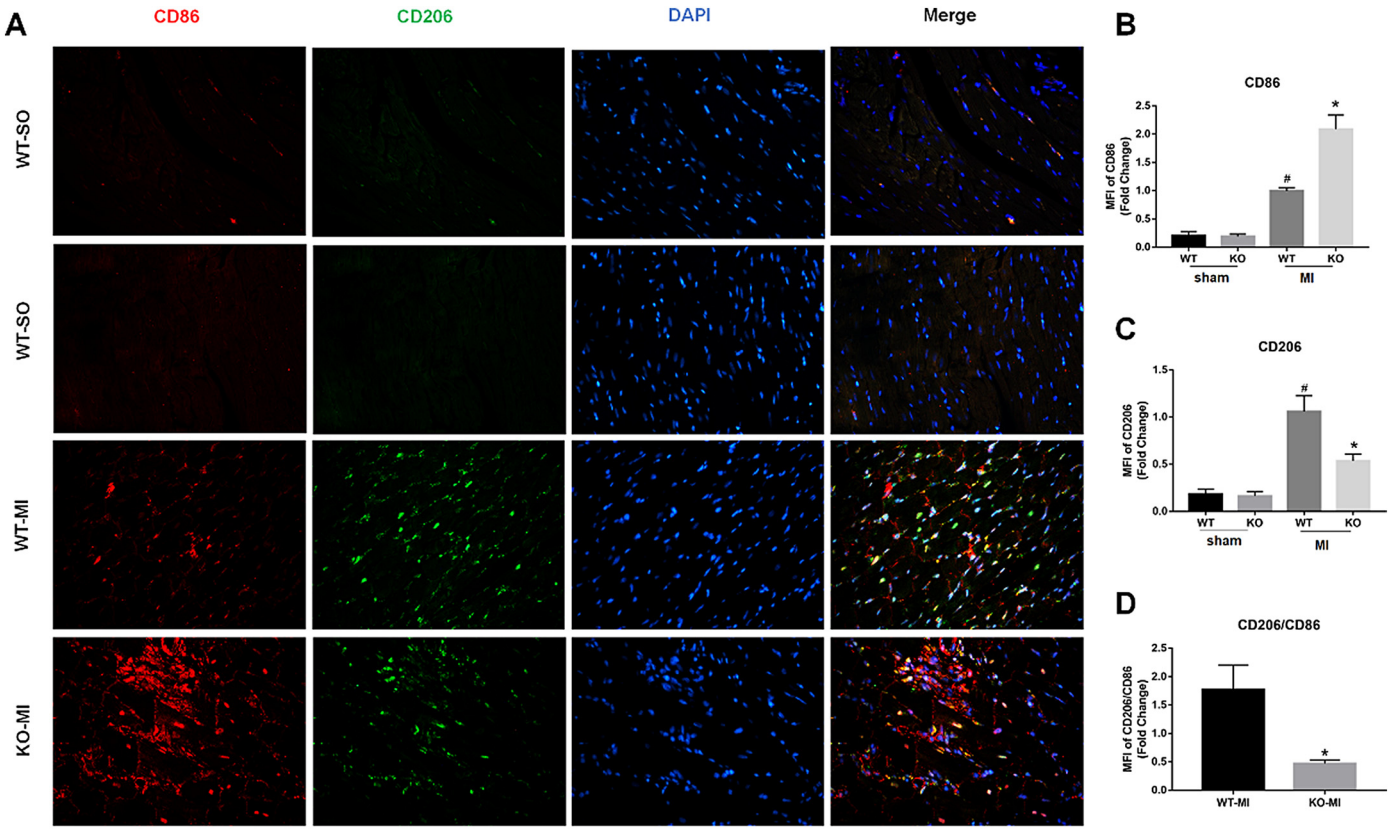

Fig. 5. KDM3A knockout inhibits macrophage polarization from the M1 to the M2 subtype and aggravates inflammatory responses post MI.
(A) Double immunofluorescence staining of CD86 (red) and CD206 (green) on macrophages in vivo. The nuclei were stained with DAPI (blue) (×200). (B-D) Quantitative analysis of the relative MFI of CD86 and CD206 by Image ProPlus software and statistical analysis of the ratio of CD206/CD86 ($n = 4$, $^*P < .05$ vs. WT-MI, $\#P < .05$ vs. sham). Data are expressed as the mean ± standard deviation. SO: sham operation; MI: myocardial infarction; WT: wild-type; KO: knockout; MFI: mean fluorescence intensity. (For interpretation of the references to colour in this figure legend, the reader is referred to the web version of this article.)

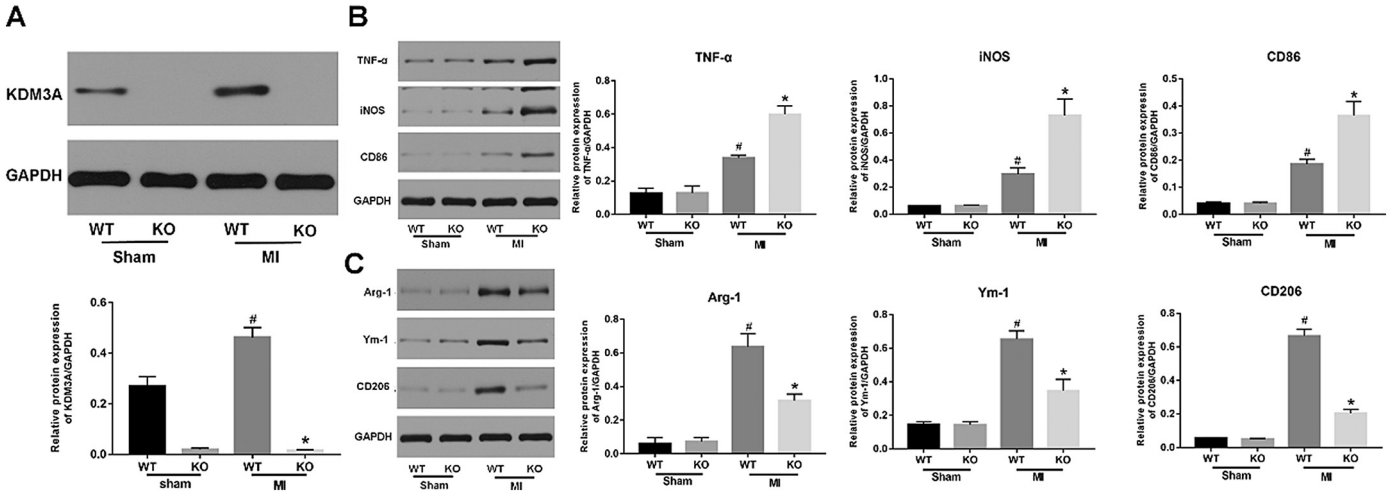

Fig. 6. KDM3A knockout increases M1 but suppresses M2 macrophage polarization in vivo.
(A) KDM3A protein expression was determined by western blot analysis ($n = 3$, $^*P < .05$ vs. WT-MI, $\#P < .05$ vs. sham) (B) The protein expression of the M1 macrophage markers TNF-α, iNOS, and CD86 at 7 days post MI by western blot analysis ($n = 3$, $^*P < .05$ vs. WT-MI, $\#P < .05$ vs. sham.) (C) The protein expression of the M2 macrophage markers Arg-1, Ym-1, and CD206 at 7 days post MI by western blot analysis ($n = 3$, $^*P < .05$ vs. WT-MI, $\#P < .05$ vs. sham). Data are expressed as the mean ± standard deviation. TNF-α: tumor necrosis factor alpha; iNOS: inducible nitric oxide synthase; Arg-1: arginase-1; GAPDH: glyceraldehyde 3-phosphate dehydrogenase Fig. 8).

KO rat cardiac tissue(Fig. 6A), and in Fig. 6B, the M1 macrophage surface marker protein (CD86) expression and inflammatory factor (TNF-α and iNOS) secretion in the KO-MI group were higher than those in the WT-MI group, while the M2 macrophage surface marker protein (CD206) expression and anti-inflammatory factor(Arg-1 and Ym-1) secretion were lower (Fig. 6C). Therefore, KDM3A inhibition promotes the polarization of macrophages to an inflammatory phenotype but reduces the polarization of macrophages to a reparative and protective phenotype in the infarcted zone during the early phase of MI.

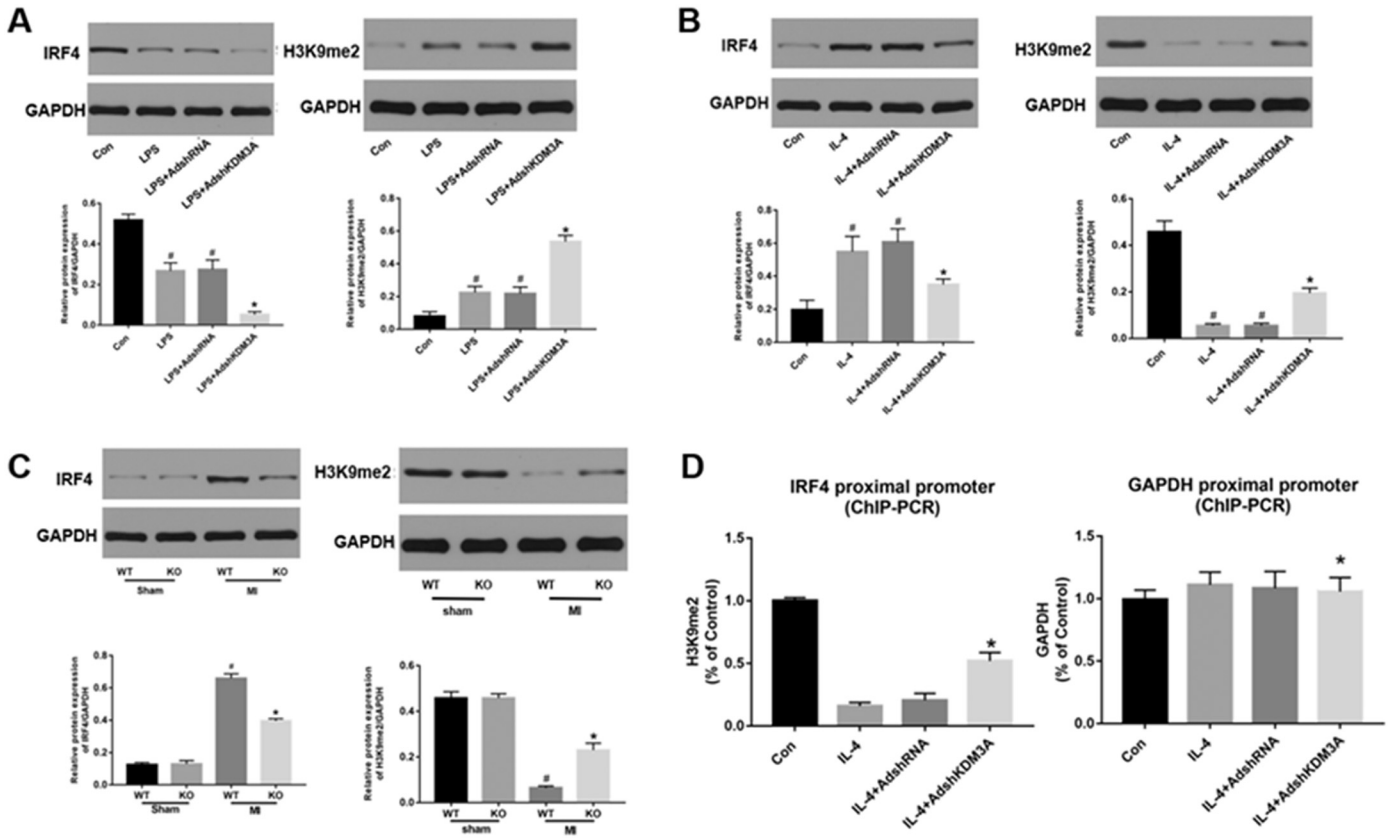

Fig. 7. KDM3A inhibition modulates macrophage polarization to aggravate post-MI injuries and accelerates adverse ventricular remodeling via an IRF4 signaling pathway. (A–B) Western blot analysis of the protein expression of IRF4 and H3K9me2 on BMDMs stimulated with medium alone (Con), LPS (1 μg/ml) for M1 polarization, and IL-4 (20 ng/ml) for M2 polarization in vitro ($n = 3$, $^*P < .05$ vs. LPS + AdshRNA/IL-4 + AdshRNA or LPS/IL-4, $\#P < .05$ vs. Con). (C) Western blot analysis of the protein expression of IRF4 and H3K9me2 on macrophages at 7 days post MI ($n = 3$, $^*P < .05$ vs. WT-MI, $\#P < .05$ vs. sham). (D) ChIP assays were performed to verify the H3K9me2 levels in the process of inducing polarization of macrophages after the downregulation of KDM3A protein level. Data are expressed as a percentage of Control group ($n = 3$, $^*P < .05$ vs. Con). Data are expressed as the mean ± standard deviation. SO: sham operation; MI: myocardial infarction; WT: wild-type; KO: knockout; LPS: lipopolysaccharide; IL-4: interleukin-4; IRF4: interferon regulatory factor 4; H3K9me2: H3 lysine 9 di-methylation.

3.6. KDM3A inhibition modulates macrophage polarization via the IRF4 pathway

IRF4 has been demonstrated to regulate macrophage polarization in the inflammatory response of many pathological processes, including post MI [22,23]. To test whether KDM3A inhibition modulates the activities of IRF4, western blotting was used to detect the expression of IRF4 (Fig. 7). Isolated BMDMs were polarized into MI (LPS) or M2 (IL-4) macrophages for 24 h prior to adenovirus transfection, and the hearts of each group were harvested at day 7 post MI. The western blot analysis showed that LPS downregulated the levels of IRF4 and IL-4 and upregulated the levels of IRF4. After transfection with AdshKDM3A, the level of IRF4 was downregulated both in LPS stimulation and IL-4 stimulation (Fig. 7A–B). In addition, the level of IRF4 was downregulated in the KO-MI group compared with the WT-MI group (Fig. 7C). These data indicate that KDM3A inhibition shifted macrophage polarization away from the M2 phenotype and may be closely correlated with IRF4 silencing.

Furthermore, H3K9me2, as a specifically target of KDM3A could verified the attenuate degree of histone methylation of KDM3A. In Fig. 7, western blot analysis showed that downregulating the expression of KDM3A not only decreasing the protein level of IRF4, but increasing H3K9me2 level both in vitro and vivo. Next, following experiments were designed by ChIP-PCR assay to further substantiate the underlying mechanism, whether IRF4 silence in connection with the epigenetic activation of H3K9me2 during the downregulation of KDM3A protein level in the process of inducing polarization of macrophages. ChIP-PCR revealed that H3K9me2 level was increased on the IRF4 gene proximal promoter in the AdshKDM3A group compared with the AdshRNA group. Meanwhile, there were no markedly differences on the GAPDH promoter which was regarded as a control (Fig. 7D). Our data unanimous indicated that KDM3A deficiency epigenetically influences the transcription of IRF4 by enhancing H3K9me2 accumulation on the IRF4 gene proximal promoter region.

4. Discussion

Previous studies suggested that even if treated with reperfusion surgery in a timely manner, some patients with MI will still suffer the consequences of cardiac dysfunction or even heart failure [2,3]. One of the important reasons for this finding is that the patient's early inflammatory response is too long, which delays the repair and reconstruction of the myocardium. At the same time, the excessive secretion of inflammatory factors promotes the proliferation of fibroblasts and collagen deposition, resulting in left ventricular dilatation and excessive scar formation [1]. Therefore, timely suppression of the excessive inflammatory response has a profound impact on the progress and quality of remodeling after myocardial infarction. Although the role of KDM3A in regulating the function of smooth muscle cells has been confirmed previously, its involvement in macrophages and potential mechanisms post MI remain uncertain. Our present study suggested that KDM3A is a novel therapeutic candidate that could affect the process of inflammation by regulating the phagocytosis and migration capability of macrophages and influencing the phenotypic

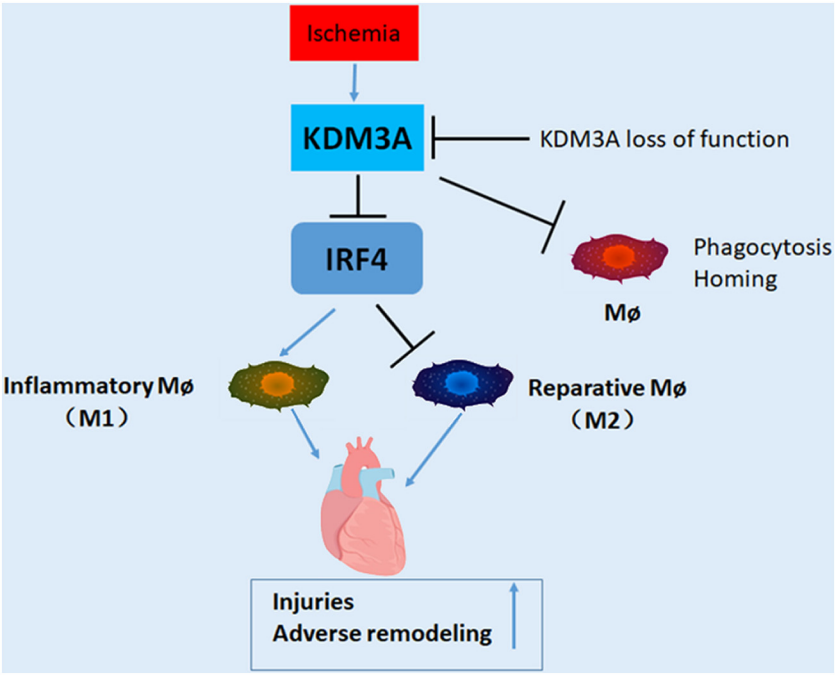

Fig. 8. The function of KDM3A inhibition in post-infarction repair and remodeling.
KDM3A inhibition attenuates macrophage phagocytosis and migration capability. Furthermore, KDM3A inhibition promotes the polarization of macrophages to an inflammatory phenotype but reduces the polarization of macrophages to a reparative and protective phenotype to aggravate post-MI injuries and accelerates adverse ventricular remodeling via an IRF4 signaling pathway.

polarization of macrophages, thus influencing the prognosis of myocardial infarction and adverse left ventricular (LV) remodeling. Additionally, mechanistic studies demonstrated that KDM3A deficiency clearly decreased IRF4 expression by enhancing H3K9me2 accumulation on the proximal promoter region. To the best of our knowledge, our present study is the first report to verify the effects of KDM3A inhibition on macrophages and suggests a promising therapy to treat post-MI injuries.

Following myocardial ischemia injury, a large number of activated mononuclear phagocyte system and infiltrate the ischemic area, resulting in aseptic inflammation of the myocardium. In the first 3 days, inflammatory monocytes transform into the M1 macrophages, secrete proteases and cytokines, clear necrotic cell fragments, and degrade and reconstruct the ECM. At later stages (~3–7 days), the proinflammatory M1 phenotype is transformed into the reparative M2 phenotype, which promotes collagen deposition, scar repair and neovascularization [2,25]. Macrophages, as immune cells, are different from other immune cells. They are transformed into different phenotypes according to the needs of the environment and play different roles. Macrophages (M0) in the stationary state of cardiac homeostasis are transformed into macrophages (M1) by the classical activated state and then are transformed into anti-inflammatory repair macrophages (M2) after the inflammation subsides [5,25]. Therefore, the degree and time of transformation between macrophage phenotypes are crucial to the outcome and prognosis of myocardial ischemic infarction injury.

In recent years, researchers have attempted to explain some biological phenomena through epigenetics. Histone modification is an important part of epigenetic modification, which regulates gene transcription by changing chromatin remodeling, thus regulating cell function [8,26]. Adequate evidence suggests that KDM3A is an epigenetic regulator and plays a variety of biological roles by removing the suppressive histone mark H3K9me2 in cardiovascular disease. KDM3A regulates the function of smooth muscle cells through the MAPK/NF-κB signaling pathway, and a loss of KDM3A could depress ROS generation, apoptosis and the inflammatory response [14]. In addition, KDM3A is involved in regulating vascular remodeling in diabetes mellitus via AGTR1 and ROCK2 pathways and the underlying mechanisms were KDM3A controlled the H3K9me2 accumulation on the gene proximal promoter region to influence the transcription of AGTR1 and ROCK2. KDM3A knockout reduces collagen deposition but exacerbates inflammatory and oxidative stress [15], KDM3A upregulation promotes left ventricular hypertrophy and pathological fibrosis by activating Timp1 transcription [13]. In addition to participating in cardiovascular disease, KDM3A also plays a significant role in regulating macrophage polarization and function. Tsuyoshi and coworkers convincingly demonstrated that JMJD1A (KDM3A) inhibition suppressed CD31 vascular formation markers and reduced the infiltration of CD11b monocytes and F4/80 macrophages in tumor progression [27]. Simultaneously, it had been reported that Jumonji domain-containing-3 (JMJD3), a histone 3 lysine 27 (H3K27) demethylase, could activate M2 macrophage polarization through the JMJD3-IRF4 axis [18]. Although existing studies have indicated that KDM3A could regulate macrophages in tumor diseases, it has not been determined whether KDM3A plays a cardioprotective role in regulating macrophages in cardiovascular diseases. Macrophages repair myocardial infarction through inflammatory modulation; however, KDM3A can intervene in inflammatory responses during the pathological process of cardiovascular diseases. Based on the analysis of the above research, we questioned whether KDM3A would play a significant role in macrophage polarization post MI.

To examine this question, in the study presented here, we confirmed that KDM3A affected the process of inflammation by regulating the major function and phenotypic polarization of macrophages, thus affecting the prognosis of myocardial infarction and adverse left ventricular (LV) remodeling. In vitro, inhibition of the expression of KDM3A in BMDMs led to a decrease in phagocytosis and attenuated the capability of macrophages to migrate to respond to the chemokines of myocardial cell necrosis (Fig. 2), which suggested that KDM3A inhibition might contribute to the loss of macrophage homing to injured tissues and the inefficient clearance of cellular debris. KDM3A deficiency led to an increase in the secretion of proinflammatory cytokines and more differentiation of macrophages into the M1 phenotype under LPS stimulation (Fig. 3C), but the capability of macrophages to differentiate into the M2 phenotype was inhibited under IL-4 stimulation (Fig. 3E). Furthermore, our results showed that there was a significant difference in the infiltration of M1 and M2 macrophages between the KO-MI and WT-MI groups 7 days post MI (Fig. 5). Meanwhile, we observed more M1 macrophage ($CD86^+$) infiltration and a higher M1/M2($CD86^+/CD206^+$) ratio in the myocardial infarction area of KO-MI rats. By contrast, WT-MI rats were more infiltrated with M2

macrophages ($CD206^+$) (Fig. 5). Moreover, the secretion trends of M1- or M2-related phenotypic markers and cytokines in the two groups were consistent in vitro (Fig. 6). These observations consistently indicate that inhibition of KDM3A could lead to the polarization of macrophages toward the proinflammatory M1 phenotype and a failure to convert into the repaired M2 phenotype in a timely manner during the inflammation-reparative transition phase. As shown in Fig. 4, ventricular dilatation, fibrosis and cardiac function in the KO-MI group were worse than those in the WT-MI group at 7 days and one month post MI (Fig. 3). These findings indicated that KDM3A inhibition could contribute to aggravating adverse left ventricular remodeling after MI.

To explore the potential mechanism of KDM3A regulation of macrophages, we found a variety of possible mechanisms to regulate the immune response, among which the IRF family attracted our attention. The interferon regulatory factor family is a group of transcription factors widely expressed in various tissues and organs that not only participate in signal transduction through pattern recognition receptors [28] but also bind to the promoter region of the type I IFN gene to regulate the activity and function of macrophages [29]. As one of the IRF family members, IRF4 mainly acts on the immune system, including regulating the polarization of M1 and M2 macrophages [30]. Pohl et al. showed that $CD103^+CD11b^+$ dendritic cells were required for the activation of monocytes and macrophages to produce iNOS via the IRF4 signaling pathway [31]. The studies of Sapoh et al. [32] and Smith et al. [33] showed that IRF4 not only acts as a transcription factor for M2 activation but also plays a key role in metabolic reprogramming in the M2 activation process, especially glucose metabolism, which participates in M2 activation. UDP-Glc-NAc, as a substrate biomarker of M2 glycosylation is produced in the process of glycolysis. In addition, glycolysis helps to induce the gene expression of M2 [33,34]. These previous studies suggested that IRF4 had a regulatory impact on macrophage polarization. In addition, in the present study, after BMDMs were transferred by AdshKDM3A, we detected the expression of KDM3A protein by western blot analysis and found that, concomitant with the changes in KDM3A, IRF4 also changed. Furthermore, a previous study demonstrated the relationship between KDM3A and IRF4 core promoter regions, determining that KDM3A, through adjusting H3K9me1 and H3K9me2 methylation, can directly regulate the expression of IRF4 [32]. Thus, we further explored whether IRF4 was the downstream effector of the KDM3A-dependent pathway post MI by western blots analysis and the ChIP-PCR assay. Indeed, western blot analysis showed that downregulating the expression of KDM3A not only weakened the expression of IRF4 and decreased the capability of macrophages to polarize to the M2 phenotype, but increasing H3K9me2 level both in vitro and vivo. (Fig. 7A–C). Furthermore, ChIP-PCR revealed that H3K9me2 level was increased on the IRF4 gene proximal promoter in the AdshKDM3A group compared with the AdshRNA group. Therefore, KDM3A provides a therapeutic strategy to modulate macrophage polarization to aggravate post-MI injuries and accelerates adverse ventricular remodeling by enhancing H3K9me2 accumulation on the IRF4 gene proximal promoter region, epigenetically influencing the transcription of IRF4. (Fig. 7C). Besides, in the present study, we also have several lacunae we don't investigate. Whether there have other epigenetic modification mechanisms to modulate macrophage polarization, and what are the specific downstream or upstream effector molecules regulated by the KDM3A-H3K9me2-IRF4 pathway. These lacunae need us to further investigate in the next experiment.

5. Conclusion

In conclusion, our results revealed that KDM3A was critical for mediating macrophage polarization, phagocytosis and migration to participate in the cardiac repair process and left ventricular remodeling post MI. We also found that IRF4 was a downstream effector of the KDM3A-dependent pathway. These findings not only indicated that targeting KDM3A to modulate macrophage polarization via the IRF4 signaling pathway in the infarcted heart might be a promising novel therapeutic strategy for cardiac repair and function but also suggested that skewing macrophage polarization toward a reparative phenotype might be a pivotal treatment post MI.

Declaration of Competing interest

The authors declare no conflicts of interests.

Acknowledgments

This study was supported by the National Natural Science Foundation of China (81570331) and Nature Science Foundation of Hubei Province(2018CFB240).

Appendix A. Supplementary data

Supplementary data to this article can be found online at https://doi.org/10.1016/j.cellsig.2019.109415.

References

[1] B.R. Weil, S. Neelamegham, Selectins and immune cells in acute myocardial infarction and post-infarction ventricular remodeling: pathophysiology and novel treatments, Front. Immunol. 10 (2019) 300.
[2] S.D. Prabhu, N.G. Frangogiannis, The biological basis for cardiac repair after myocardial infarction: from inflammation to fibrosis, Circ. Res. 119 (1) (2016) 91–112.
[3] M.G. Sutton, N. Sharpe, Left ventricular remodeling after myocardial infarction: pathophysiology and therapy, Circulation. 101 (25) (2000) 2981–2988.
[4] P. Panizzi, F.K. Swirski, J.L. Figueiredo, P. Waterman, D.E. Sosnovik, E. Aikawa, et al., Impaired infarct healing in atherosclerotic mice with Ly-6C(hi) monocytosis, J. Am. Coll. Cardiol. 55 (15) (2010) 1629–1638.
[5] C. Troidl, H. Mollmann, H. Nef, F. Masseli, S. Voss, S. Szardien, et al., Classically and alternatively activated macrophages contribute to tissue remodelling after myocardial infarction, J. Cell. Mol. Med. 13 (9B) (2009) 3485–3496.
[6] M. Bujak, M. Dobaczewski, C. Gonzalez-Quesada, Y. Xia, T. Leucker, P. Zymek, et al., Induction of the CXC chemokine interferon-gamma-inducible protein 10 regulates the reparative response following myocardial infarction, Circ. Res. 105 (10) (2009) 973–983.
[7] R.J. Klose, Y. Zhang, Regulation of histone methylation by demethylimination and demethylation[J], Nat. Rev. Mol. Cell Biol. 8 (4) (2007) 307–318.
[8] T. Nakatsuka, K. Tateishi, Y. Kudo, K. Yamamoto, H. Nakagawa, H. Fujiwara, et al., Impact of histone demethylase KDM3A-dependent AP-1 transactivity on hepatotumorigenesis induced by PI3K activation, Oncogene. 36 (45) (2017) 6262–6271.
[9] S. Ramadoss, G. Guo, C.Y. Wang, Lysine demethylase KDM3A regulates breast cancer cell invasion and apoptosis by targeting histone and the non-histone protein p53[J], Oncogene. 36 (1) (2017) 47–59.
[10] S. Ramadoss, S. Sen, I. Ramachandran, S. Roy, G. Chaudhuri, R. Farias-Eisner, Lysine-specific demethylase KDM3A regulates ovarian cancer stemness and chemoresistance[J], Oncogene. 36 (11) (2017) 1537–1545.
[11] D.S. Jiang, X. Yi, R. Li, Y.S. Su, J. Wang, M.L. Chen, et al., The histone methyltransferase Mixed Lineage Leukemia (MLL) 3 May play a potential role on clinical dilated cardiomyopathy, Mol. Med. 23 (2017) 196–203.
[12] G. Yang, X. Weng, Y. Zhao, X. Zhang, Y. Hu, X. Dai, et al., The histone H3K9 methyltransferase SUV39H links SIRT1 repression to myocardial infarction, Nat. Commun. 8 (2017) 14941.
[13] Q.J. Zhang, T.A.T. Tran, M. Wang, M.J. Ranek, K.M. Kokkonen-Simon, J. Gao, et al., Histone lysine dimethyl-demethylase KDM3A controls pathological cardiac hypertrophy and fibrosis, Nat. Commun. 9 (1) (2018) 5230.
[14] B.F. Zhang, H. Jiang, J. Chen, X. Guo, Q. Hu, S. Yang, KDM3A inhibition attenuates high concentration insulininduced vascular smooth muscle cell injury by suppressing MAPK/NFkappaB pathways, Int. J. Mol. Med. 41 (3) (2018) 1265–1274.
[15] J. Chen, J. Zhang, J. Yang, L. Xu, Q. Hu, C. Xu, et al., Histone demethylase KDM3a, a novel regulator of vascular smooth muscle cells, controls vascular neointimal hyperplasia in diabetic rats, Atherosclerosis. 257 (2017) 152–163.
[16] J. Weischenfeldt, B. Porse, Bone Marrow-Derived Macrophages (BMM): isolation and applications, CSH Protocol. 2008 (2008) (pdb prot5080).
[17] X. Zhang, R. Goncalves, D.M. Mosser, The isolation and characterization of murine macrophages, Curr. Protoc. Immunol. 83 (1) (2008) 1–14, https://doi.org/10.1002/0471142735.im1401s83.
[18] X. Feng, H. Qin, Q. Shi, Y. Zhang, F. Zhou, H. Wu, et al., Chrysin attenuates inflammation by regulating M1/M2 status via activating PPARgamma, Biochem. Pharmacol. 89 (4) (2014) 503–514.
[19] F. Zhang, Y. Xuan, J. Cui, X. Liu, Z. Shao, B. Yu, Nicorandil modulated macrophages activation and polarization via NF-kappab signaling pathway, Mol. Immunol. 88 (2017) 69–78.
[20] K. Nakamura, W. Fujii, M. Tsuboi, J. Tanihata, N. Teramoto, S. Takeuchi, et al., Generation of muscular dystrophy model rats with a CRISPR/Cas system, Sci. Rep. 4

(2014) 5635.
[21] Y. Cao, S. He, Z. Tao, W. Chen, Y. Xu, P. Liu, et al., Macrophage-specific IkappaB kinase alpha contributes to ventricular remodelling and dysfunction after myocardial infarction, Canadian J. Cardiol. 35 (4) (2019) 490–500.
[22] J. Wang, M. Liu, Q. Wu, Q. Li, L. Gao, Y. Jiang, et al., Human embryonic stem cell-derived cardiovascular progenitors repair infarcted hearts through modulation of macrophages via activation of signal transducer and activator of transcription, Antioxid. Redox Signal. 6 (2019).
[23] E. Wan, X.Y. Yeap, S. Dehn, R. Terry, M. Novak, S. Zhang, et al., Enhanced efferocytosis of apoptotic cardiomyocytes through myeloid-epithelial-reproductive tyrosine kinase links acute inflammation resolution to cardiac repair after infarction, Circ. Res. 113 (8) (2013) 1004–1012.
[24] D.J. Cao, G.G. Schiattarella, E. Villalobos, N. Jiang, H.I. May, T. Li, et al., Cytosolic DNA sensing promotes macrophage transformation and governs myocardial ischemic injury, Circulation. 137 (24) (2018) 2613–2634.
[25] K. Fujiu, J. Wang, R. Nagai, Cardioprotective function of cardiac macrophages, Cardiovasc. Res. 102 (2) (2014) 232–239.
[26] S. Ikeda, A. Kitadate, F. Abe, N. Takahashi, H. Tagawa, Hypoxia-inducible KDM3A addiction in multiple myeloma, Blood Advances. 2 (4) (2018) 323–334.
[27] T. Osawa, R. Tsuchida, M. Muramatsu, T. Shimamura, F. Wang, J. Suehiro, et al., Inhibition of histone demethylase JMJD1A improves anti-angiogenic therapy and reduces tumor-associated macrophages, Cancer Res. 73 (10) (2013) 3019–3028.
[28] K. Ozato, P. Tailor, T. Kubota, The interferon regulatory factor family in host defense: mechanism of action, J. Biol. Chem. 282 (28) (2007) 20065–20069.
[29] D. Savitsky, T. Tamura, H. Yanai, T. Taniguchi, Regulation of immunity and oncogenesis by the IRF transcription factor family, Cancer Immunol. Immunother.: CII. 59 (4) (2010) 489–510.
[30] C.J. Ferrante, S.J. Leibovich, Regulation of macrophage polarization and wound healing, Adv. Wound Care. 1 (1) (2012) 10–16.
[31] J.M. Pohl, S. Gutweiler, S. Thiebes, J.K. Volke, L. Klein-Hitpass, D. Zwanziger, et al., Irf4-dependent CD103(+)CD11b(+) dendritic cells and the intestinal microbiome regulate monocyte and macrophage activation and intestinal peristalsis in postoperative ileus, Gut. 66 (12) (2017) 2110–2120.
[32] T. Satoh, O. Takeuchi, A. Vandenbon, K. Yasuda, Y. Tanaka, Y. Kumagai, et al., The Jmjd3-Irf4 axis regulates M2 macrophage polarization and host responses against helminth infection, Nat. Immunol. 11 (10) (2010) 936–944.
[33] S.C. Huang, A.M. Smith, B. Everts, M. Colonna, E.L. Pearce, J.D. Schilling, et al., Metabolic reprogramming mediated by the mTORC2-IRF4 signaling Axis is essential for macrophage alternative activation, Immunity. 45 (4) (2016) 817–830.
[34] A.J. Covarrubias, H.I. Aksoylar, J. Yu, N.W. Snyder, A.J. Worth, S.S. Iyer, et al., Akt-mTORC1 signaling regulates Acly to integrate metabolic input to control of macrophage activation, eLife. 5 (2016).